DARK MATTER IN GALAXIES

K.C. Freeman
Mount Stromlo and Siding Spring Observatories
The Australian National University

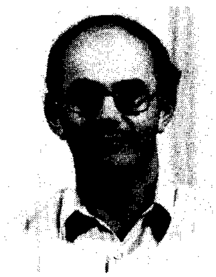

ABSTRACT

We review the observational evidence for dark matter in galaxies. From observations of the kinematics of gas in spiral galaxies and dwarf irregulars, there is not much doubt now that most of these galaxies have dark halos which are at least a few times more massive than their luminous components. Elliptical and dwarf spheroidal galaxies also appear to have massive dark halos, but for these galaxies the evidence is less direct.

1. SPIRAL GALAXIES

1.1. Structure of the dark halos

Spiral galaxies commonly have flat rotation curves, which cannot be produced by a mass distribution that follows the surface brightness distribution. The upper panel of Figure 1 shows the surface brightness distribution for the spiral galaxy NGC 3198 [1]; the lower panel shows the contributions to the rotation curve from the gas and the stellar disk (assuming that the mass to light ratio M/L of the disk is constant with radius). In Figure 1, the adopted M/L ratio for the disk is the maximum allowed by the observed rotation curve. The rotation curve for the disk fits the data well enough in the inner regions (out to about 3 scalelengths as determined from the exponential surface brightness distribution), but beyond 5 kpc the expected rotation curve from this maximum disk plus the gas lies far below the observed rotation curve.

This situation is typical of most spirals with measured rotation curves extending well beyond 3 scalelengths. The usual interpretation is that these galaxies have a massive dark halo which makes up the shortfall in the rotation curve. The flat shape of the rotation curves in the outer regions of spirals suggests that the radial density distribution of this dark halo goes like $\rho(r) \sim r^{-2}$ at large radius. A simple model that is often used has

$$\rho(r) = \rho_\circ/[1 + (r/a)^2] \tag{1}$$

Figure 1 shows the contribution of such a halo, scaled so that the total expected rotation curve from the disk, gas and dark halo fits the data. This maximum disk model minimises the contribution from the dark halo; models with less massive disks and more massive halos often fit just as well [2]. Even with the maximum disk model, the mass of the dark halo of NGC 3198 is about five times the mass of the luminous disk plus gas within the outermost point on the observed rotation curve.

The simple halo given by equation (1) has two scales: the core radius a and the central density $\rho_\circ$. The estimated values of these two scales from the rotation curve analysis depend on the adopted value for the disk's M/L ratio. The maximum disk models give the largest core radii and the smallest $\rho_\circ$. The typical values of $\rho_\circ$ from maximum disk solutions are in the range $\rho_\circ = 0.001$ to $0.01\ M_\odot$ for giant spirals and 0.01 to 0.1 $M_\odot$ for the smaller spirals and irregulars. The core radii for the large spirals derived from maximum disk solutions are typically 10 to 20 kpc, but could be much smaller if the maximum disk analysis is not the correct procedure [2].

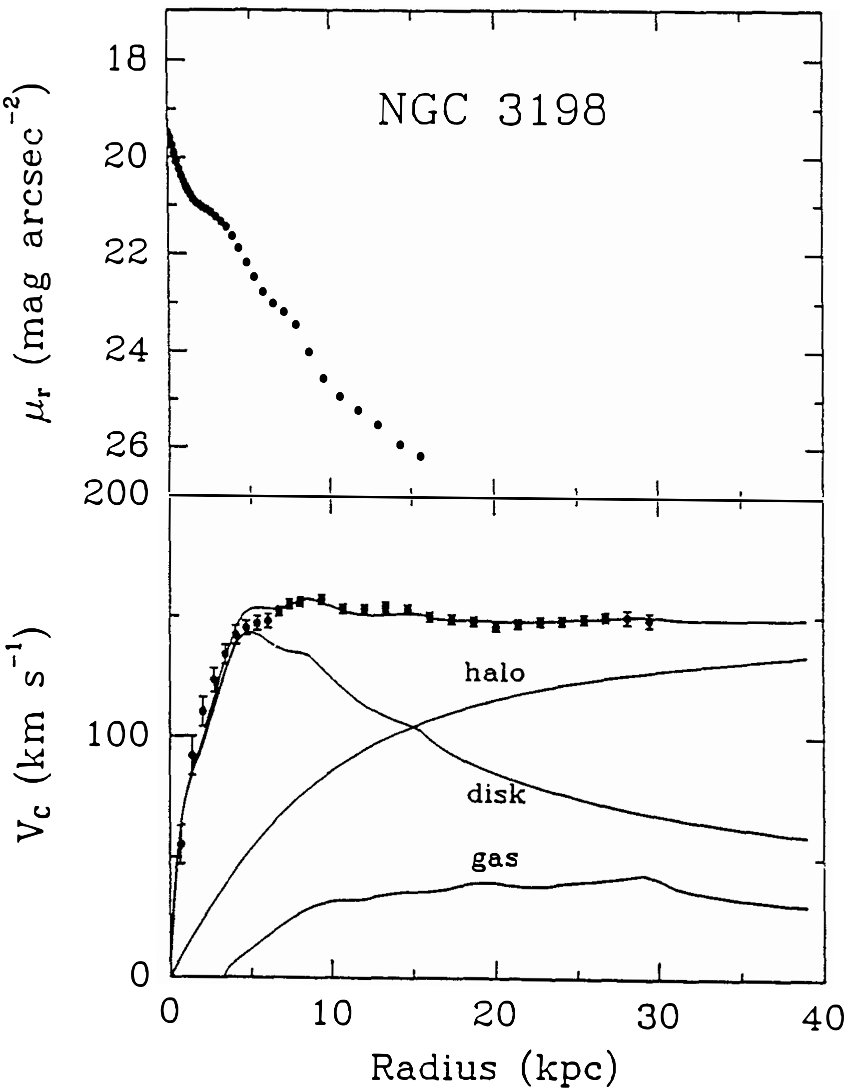

Figure 1:–Upper panel: Surface brightness distribution for NGC 3198 [1]. Lower panel: The filled symbols show the rotation curve for NGC 3198. The labelled curves show the contribution of the gas, disk and halo to the circular velocity. The total circular velocity from these three components is shown as the upper curve.

The core radius, central density and shape of the dark halos are interesting because they relate to simulations of galaxy formation . For example, Warren *et al.* [3] made simulations of a 400 Mpc^3 piece of the universe, using 10^6 particles and various perturbation spectra. In these simulations, the halos grow by dissipationless merging of smaller collapsed structures via dynamical friction and tidal stripping. They find that (i) halos tend to be more prolate than oblate, and (ii) the core radii are typically about 1 kpc for large halos with circular velocities of 250 km s^{-1}. This is much smaller than the halo core radii inferred from maximum disk analysis of rotation curves of large spirals. These results suggest that either the maximum disk solutions are not appropriate or some mechanism is needed to enlarge the cores of large spirals. This core growth may occur naturally as gas settles to a disk during the hierarchial merging: Katz and Gunn [4] showed that the settling gas can transfer more than 50% of its original angular momentum to the dark halo.

The shape of the dark halos are not yet well constrained by observation. The flaring of the gas layer observed in edge-on spirals gives some information about the shape of the potential in the outer parts of these systems. A recent study by Maloney [5] concludes that dark matter distributions as flat as the disk can probably be excluded. In polar ring galaxies, it is possible to estimate the shape of the dark matter distribution from the kinematics of gas and stars in the two perpendicular planes of the stellar disk and the polar ring. Recent results for the system NGC 4650A [6,7] are consistent with a fairly flat (E6) dark halo.

1.2. Maximum Disks

We return now to the question of the maximum disk analysis of rotation curves. This question has been widely discussed (see the review by Sancisi and van Albada [8]), because it is important to know whether this is the right way to proceed. Our knowledge of the structure of dark halos depends on the assumptions about the M/L ratio for the stellar disk. It also affects our view of the dynamics of the inner disk: does the disk dominate the radial potential gradient in the inner two or three scalelengths, or is it dominated even in the inner regions by the dark halo.

Analysis of the rotation curve of our Galaxy does not give a clear answer to the maximum disk question. The rotation curve in the inner regions is not well determined, and the relative contributions to the potential field from the disk and the bulge are difficult to assess. Different studies indicate that the surface density of a maximum disk near the sun would lie somewhere in the range 70 to 130 $M_{\odot}$ pc^{-2}, depending on the adopted mass of the galactic bulge [9,10]. Recent estimates of the local surface density, from the kinematics and distribution of stars towards the galactic poles [11,12], are in the range 50 to 80 $M_\odot$ pc^{-2}.

Swing amplifier theory for spiral structure can give some useful limits on the density of the disk, by requiring that the disk should not be so dense as to allow $m = 1$ modes. Athanassoula *et al.* [13] made maximum disk fits to a large sample of rotation curves, with the extra constraint of "no $m = 1$ amplification". They found that their fits (i) are consistent with almost all of their galaxies, (ii) are compatible with the $m > 2$ spirals seen in the outer parts of some of their galaxies, and (iii) give M/L ratios for the disks that are mostly within 20% of the unmodified maximum disk values.

Another useful guide to the M/L ratio of the disk comes from optical rotation curves in the inner few scalelengths of the disk. Some galaxies show wiggles in their optical rotation curves; these wiggles correspond to structure in the surface brightness profiles. If the maximum disk models are correct, then it should be possible to reproduce the wiggles by computing the rotation curve expected from the surface brightness distribution, assuming that the M/L ratio in the disk is constant. Kalnajs [14] was the first to show that this works; his computed rotation curves followed the detailed structure in the observed rotation curves.

Buchhorn and Mathewson [15] have recently analysed optical rotation curves of 552 spirals. The expected rotation curves were computed from their I-band CCD surface photometry, which minimises the effects of internal absorption and regions of young population in the disks. Their galaxies show a wide variety of rotation curve morphology, extending from flat rotation curves to almost solid body rotation. For most of their sample (> 97%), the calculated rotation curves are an excellent fit to the data. Figure 2 shows the good fits for two galaxies with prominent wiggles in their rotation curves. The good fits in these systems are particularly significant for the maximum disk question, because there are two velocity scales (the overall scale of the rotation curve and the scale of the wiggles) to fit with only one parameter (the M/L_I ratio). The success of their fits for this large sample, including some systems with wiggly rotation curves, suggests that either

- the disk dominates the radial potential gradient in the inner few scalelengths of most disk galaxies, or
- the detailed density distribution of the dark halo mimics the surface density structure in the disk (but the fine structure in the halo must be more prominent than in the disk because the gravitational effects of the halo structure are diluted by its probable spheroidal shape).

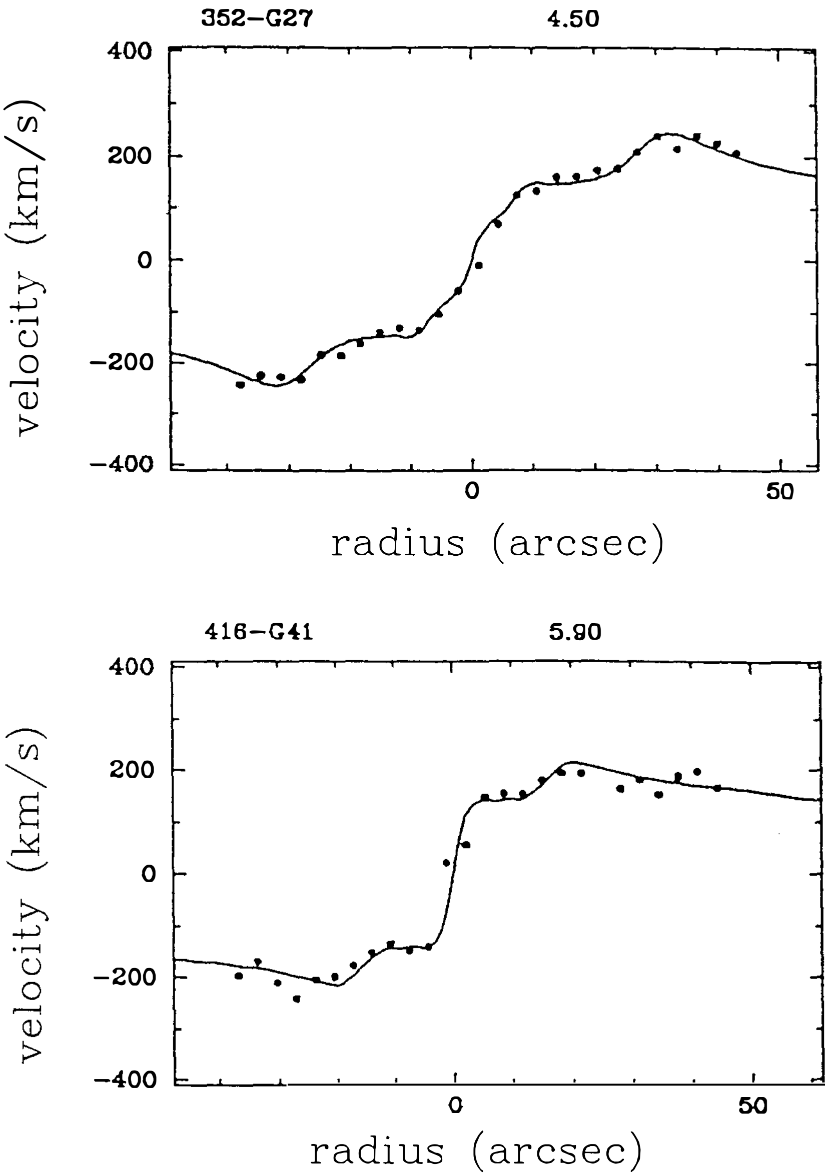

Figure 2:–Two examples of galaxies with wiggly rotation curves from Buchhorn and Mathewson [15]. See text for explanation. Galaxy identification and disk M/L ratio are shown above each panel.

Their sample includes galaxies with rotational velocities from about 40 to 350 km s^{-1}, but they find no trend of the disk's M/L_I ratio with rotational velocity. This indicates that, for most galaxies, the contribution that the halo makes to the inner rotation curve remains small as we go from the largest to the smallest spirals. However, there are a few galaxies (about 3%) for which the calculated rotation curves do not fit the data: usually the observed rotation curves show less shear than the curves expected from the surface photometry. For these few galaxies, it seems likely that the dark halo *is* making a significant contribution to the gravitational field in the inner regions of the disk.

1.3. The Dark Halo of our Galaxy

For our Galaxy, three methods are used to estimate the enclosed mass $M(R)$ within some radius R: (i) the rotation curve, (ii) the random velocities of distant halo stars and satellite galaxies, and (iii) timing arguments. From the inner rotation curve and the adopted structure of the disk and bulge, the total mass of the luminous component (disk and bulge) is at most about 9×10^{10} $M_\odot$ [9,10].

The rotation curve of the Galaxy is known to be flat out to $R \approx 17$ kpc, and the enclosed mass $M(17 \text{ kpc}) = 2 \times 10^{11}$ $M_\odot$ [16]. For the distant halo stars and satellites, the distribution of rv^2 provides a mass estimator [17], where r is the distance of the object and v its radial velocity. From the halo stars, $M(70 \text{ kpc}) = (8 \pm 3) \times 10^{11}$ $M_\odot$ [18]. The satellites give $M(150 \text{ kpc}) = (12 \pm 3) \times 10^{11}$ $M_\odot$ [19]. The timing arguments use the present separation and relative velocity of M31 and the Galaxy [20] to estimate the total mass of the M31/Galaxy system, assuming that their initial separation was small and adopting some age for the universe. M31 is about 710 kpc from the Galaxy and has a galactocentric radial velocity of -118 km s^{-1}. If the age of the universe is 18 Gyr, then the mass of the Galaxy is $(13 \pm 2) \times 10^{11}$ $M_\odot$. A similar argument using the dwarf galaxy Leo I at a distance of about 230 kpc gives $(12 \pm 2) \times 10^{11}$ $M_\odot$. These estimates assume radial orbits, so are lower limits.

In summary, the data at large R consistently indicate that the Galactic mass distribution follows

$$M(R) \approx 10^{10} \times R(\text{kpc})\ M_\odot \qquad (2)$$

with a total mass of about 10^{12} $M_\odot$. This is consistent with a flat rotation curve extending out to about 100 kpc from the galactic center. The mass of the dark halo of our Galaxy is then about ten times the mass of the luminous matter.

We should mention here the three microlensing experiments that are in progress now in Chile and Australia. These are aimed at detecting dark matter objects in the galactic halo. For example, the MACHO experiment (a collaboration between the Lawrence Livermore National Laboratory, the Center for Particle Astrophysics at the University of California, Berkeley, and Mount Stromlo and Siding Spring Observatories) uses a large CCD camera and the dedicated 50-inch telescope at Mt Stromlo to monitor about 10^7 stars in the LMC and SMC (and a similar number in the galactic bulge) for brightness fluctuations due to microlensing by intervening dark matter objects. The experiment is sensitive to dark matter objects in the mass range $2.10^{-8} \lesssim M \lesssim 200\ M_{\odot}$. At the lower mass limit, the Einstein ring of the lensing object is comparable in diameter to the radius of a distant main sequence star. At the upper limit, the typical timescale of a microlensing event is similar to the likely duration of the experiment.

1.4. Conclusion for Spirals

There seems little doubt now that spirals have extended dark halos with masses of order 3 to 10 times the mass of their luminous components. The rotation curve studies described above support the maximum disk concept in most spirals; for the Milky Way the situation is still unclear. Before leaving the spirals, we should mention three particular problems.

1) The conspiracy: for galaxies with flat rotation curves, the maximum disk solutions mean that the rotation curve contributions from the disk and the dark halo have similar amplitudes, as in Figure 1 for NGC 3198. The reason for this is not yet properly understood. Recently Casertano and van Gorkom [21] and Carignan and Puche [22] studied some disk galaxies for which the rotation curves decline with increasing radius. These are usually fairly compact spirals in which the peak of the rotational velocity contribution from the disk is larger than the maximum rotational velocity for the halo, so in these systems there is no conspiracy. A dark halo is still essential to produce the observed rotation curve in their outer parts.
2) If the maximum disk concept is correct, then the disk dominates the radial potential gradient over the inner two to three scalelengths where the optical rotation curves can be measured. The optical rotation curves typically end (*i.e.* the HII region emission ends) close to the radius at which the disk's contribution to the rotation curve begins to decline and the halo begins to contribute significantly to the radial potential gradient. This observation requires some explanation. We note that, at this radius in most galaxies, the dark halo does not yet dominate

the potential gradient in the radial direction and certainly not in the vertical direction.

3) The dark halo is seen most clearly in galaxies for which the HI distribution extends out to many disk scalelengths. Several authors, most recently Carignan [23] have pointed out that the ratio $\sigma_{HI}/\sigma_{dark}$ of the directly observed surface density of HI to the inferred surface density of the dark halo is roughly constant with radius in these galaxies. Is this an important clue to the nature of dark matter, or is it simply a selection effect ?

2. THE DWARF IRREGULAR GALAXIES

HI synthesis observations of dwarf irregular galaxies give virial mass estimates from the HI profile width, assuming that the HI is in equilibrium. These estimates [24] show that the low luminosity dwarfs ($M_B > -12$) have M/L ratios $\gtrsim 12$ and are likely to have significant dark matter fractions. The brighter dwarfs ($-14.5 < M_B < -12$) have lower M/L ratios, around 3. These lower M/L values tell us little about the dark matter content, because the HI in these systems is often no more extended than the light distribution; the low M/L values just mean that the inner regions of these brighter dwarfs are not dark matter dominated. Two of the well studied dwarf irregulars are particularly interesting.

The first is DDO 154 [25]. This dIrr galaxy has $M_B = -13.8$ and is immersed in an extended HI envelope. Its rotation curve extends out to 15 disk scalelengths and shows that the dark halo dominates the gravitational field at almost all radii; this system is an extreme example of no conspiracy (see §1.4).

The second is GR8 [26]. In this very small system ($M_B = -10.6$), the gas is supported by random motions. Its rotation is small and disorderly (recall that the rotational velocity $\propto$ luminosity$^{1/4}$). However it is still possible to make a fairly straightforward estimate of the enclosed mass $M(R)$. The HI synthesis observations show that the HI velocity dispersion is constant with radius, at about 10 km s^{-1}, and the HI surface density distribution is very close to gaussian: $\mu_{HI} \propto \exp(-R^2/2h^2)$, where h is the scalelength. Assuming that the HI density distribution is spherical, then the volume density distribution of the HI is also gaussian and the equation of hydrostatic equilibrium takes the simple form $GM(R)/R^2 = c^2R/h^2$, where c is the random velocity of the HI. Out to the edge of the observable HI, the gas mass is $2.10^6\ M_\odot$, the stellar mass is $3.10^6\ M_\odot$, the total mass is $4.10^7\ M_\odot$, and the M/L ratio is 15. The hydrostatic equilibrium equation for this gaussian HI distribution with its isothermal turbulent velocity shows that the enclosed mass $M(R) \propto R^3$; *i.e.*

the HI component of GR8 lies in the approximately uniform density core of its dark halo. This is independent evidence for a core in a dark halo. The density in this core is about 0.07 $M_\odot$ pc^{-3}, which is much higher than the typical value for spirals ($\lesssim 0.01$ $M_\odot$ pc^{-3}) and for DDO 154 (0.016 $M_\odot$ pc^{-3})

3. THE DWARF SPHEROIDAL GALAXIES

These systems have very little gas, very low surface brightness (typically 0.1 of the night sky) and masses of about 10^6 to 10^7 $M_\odot$. For the dwarf spheroidal companions of the Galaxy, the M/L ratios are estimated by using star counts to measure the surface brightness distribution $I(R)$ and radial velocities of individual stars to measure the velocity dispersion $\sigma(R)$. If the mass follows the light, and the system is spherical, isotropic and has a homogeneous core, then the central M/L ratio is given by $M/L = 9\eta\sigma^2_{obs}(0)/2\pi GI(0)R_c$, where $\sigma_{obs}(0)$ is the observed central velocity dispersion, R_c is the half-peak-brightness radius, $I(0)$ is the central surface brightness and $\eta \approx 1$ (see ref. 24). Several of these dwarf spheroidal systems have now been studied. Two of them (Carina and Sculptor) have $M/L \approx 5$ which provides no clear result on their dark matter content. For three others (Fornax, Draco and Ursa Minor) there is strong evidence now that dark matter contributes significantly to the potential gradient in the inner regions.

Fornax [27] has an absolute magnitude $M_V = -12.6$. There is some uncertainty in its $I(R)$ distribution from different sources, and also in its velocity dispersion (depending on whether marginal members are included). The velocity dispersion is in the range 10 to 14 km s^{-1} and the central M/L ratio is between 9 and 15. The central density is 0.07 ± 0.03 $M_\odot$ pc^{-3}.

Draco and Ursa Minor [28] are very small systems, with $M_V \approx -8.5$. Their velocity dispersions are 9 ± 2 and 11 ± 2 km s^{-1} respectively. If their mass follows the light, then their central densities have very high values, about 1.0 $M_\odot$ pc^{-3}, and their M/L ratios are between 60 and 80. These values are lower by about a factor 2 if the dark matter is much more extended than the light.

4. DARK MATTER IN ELLIPTICALS

Elliptical galaxies usually have no HI at large radii (there are some exceptions: see below), so other dynamical tracers are used. These include the integrated starlight, the hot X-ray emitting gas, globular clusters and planetary nebulae, and we give a brief discussion of these different tracers.

4.1. Integrated Light

The radial equilibrium of elliptical galaxies is primarily between gravity and the pressure gradient associated with the velocity dispersion. In most ellipticals, rotation is less important. The momentum equation

$$\frac{\partial \Phi}{\partial R} = \frac{V_\varphi}{R} - \sigma_R^2 \Big\{ \frac{\partial \log \rho \sigma_R^2}{\partial R} + \frac{1}{R}(1 - \frac{\sigma_\varphi^2}{\sigma_R^2}) \Big\} \tag{3}$$

can be used to estimate the total enclosed mass within radius R from measurements of the line of sight components of the velocity dispersion σ and the mean rotation V_φ. However the observations do not yet reach into the outer regions ($r \gtrsim 2r_e$, where r_e is the half-light radius) where dark matter would dominate the potential. There is also uncertainty about the isotropy of σ, although recent work suggests that the velocity dispersion in the outer parts of giant ellipticals is close to isotropic [29)].

4.2. Hot X-ray Gas

The extended X-ray emission from many giant ellipticals indicates the presence of hot gas ($\sim 10^7$ K). Assuming spherical symmetry, the equation of hydrostatic equilibrium

$$\frac{GM(r)}{r} = -\frac{kT(r)}{\mu m_p} \Big\{ \frac{d \log \rho}{d \log r} + \frac{d \log T}{d \log r} \Big\} \tag{4}$$

gives an estimate of the enclosed mass $M(R)$, where T and ρ are the gas temperature and density. The temperature distributions in the X-ray emitting gas are not yet well determined. Using arguments about convective stability of the hot gas, Fabian *et al.* [30)] showed that for 14 E/SO galaxies the M/L ratios within the X-ray emitting region are greater than about 70, compared to typical values of about 5 in the inner regions.

4.3. Centaurus A

Planetary nebulae [31)] and globular clusters [32)] in Cen A give independent estimates of the enclosed mass M(r) out to about 20 kpc or $4r_e$. The planetary nebulae belong to the diffuse stellar population. The kinematics of a sample of about 500 planetary nebulae show that the velocity dispersion σ decreases with increasing radius and the rotation velocity V_{rot} increases: V_{rot}/σ increases from about 0.25 at $r = r_e$ to about 1.4 at $r = 4r_e$. In contrast, the globular clusters show no systemic rotation, and in this sense are similar to the halo clusters in our Galaxy. In the inner regions of Cen A ($r < 5$ kpc), the velocity dispersions of planetary nebulae and globular clusters are similar: 141 ± 23 km s^{-1} and 130 ± 20 km s^{-1} respectively.

To estimate the enclosed mass $M(r)$ from the planetary nebulae and globular cluster data, using the momentum equation, some further assumptions are made: (i) isotropy of σ, (ii) spherical potential, and (iii) spherical density distribution $\rho(r)$ derived from the light distribution. These assumptions are obviously a bit rough. However the estimates of $M(r)$ from the globular clusters and the planetary nebulae agree very well, despite the different dynamics of these two populations. The M/L_B ratio increases from 3 at the edge of the dust lane to 15 at a radius of 20 kpc, with $M(20\ \mathrm{kpc}) \approx 3.10^{11}\ M_{\odot}$.

4.4. Globular Clusters around M87 and NGC 1399

From the kinematics of the globular clusters around the giant elliptical M87, Mould *et al.* [33] showed that the M/L_V ratio in M87 increases from 6.5 at $r = 72''$ to 31 at $r = 8'$. Grillmair *et al.* [34] measured velocities for 57 globular clusters around the giant elliptical NGC 1399 in the Fornax cluster and found again that the M/L ratio increased outwards to at least $M/L = 80$. However, in this case it is not certain whether the M/L value really pertains to the galaxy alone or partly also to the Fornax cluster of galaxies. The dynamical relationship of the globular cluster system around NGC 1399 to the Fornax cluster itself is not clear: the Fornax cluster has a relatively small velocity dispersion and the velocity dispersion of the globular clusters is similar to that of the Fornax cluster itself.

4.5. Ellipticals with Outer HI Rings

The galaxy IC 2006 is a good example of an elliptical with an outer HI ring [35]. This system has an absolute magnitude $M_B = -19.7$. From its stellar velocity dispersion, the central $M/L_B = 5 \pm 1$. From the kinematics of the outer HI ring, the M/L_B ratio within $6.5r_e$ is 16^{+4}_{-2}. Several examples of related objects all show moderate increases of M/L by 2 to 4 times within 1 to 2 Holmberg radii.

4.6. Summary for Ellipticals

All of the tracers which extend out to large enough radii in elliptical galaxies (X-ray emission, planetary nebulae in Cen A, globular clusters around Cen A, M87 and

NGC 1399, and the HI ring data for IC 2006) indicate that the M/L ratio increases from about 5 in the inner regions to values in excess of 15 in the outer regions.

5. CONCLUSION

Dark matter in galaxies is apparently ubiquitous. The ratio of dark to luminous matter out to the most distant tracer is in the range 3 to 10 for the ellipticals and large spirals, and up to about 80 for some dwarf irregulars and dwarf spirals.

REFERENCES

1) Begeman, K.G. 1989. Astron.Astrophys., 223, 47.
2) Van Albada, T.S., Bahcall, J.N., Begeman, K., Sancisi, R. 1985 Astrophys.J., 295, 305.
3) Warren, M., Quinn, P., Salmon, J., Zurek, W. 1992. Astrophys.J., in press.
4) Katz, N., Gunn, J. 1991. Astrophys.J., 377, 365.
5) Maloney, P. 1991. Contribution to Space Telescope Workshop on Dark Matter.
6) Whitmore, B.C., McElroy, D.B., Schweitzer, F. 1987. Astrophys.J., 314, 439.
7) Sackett, P.D., Sparke, L.S. 1990. Astrophys.J., 361, 408.
8) van Albada, T.S., Sancisi, R. 1986. Phil. Trans. R. Soc. Lond. A, 320, 447.
9) van der Kruit, P.C. 1987. in The Galaxy, ed G. Gilmore, R. Carswell, (Dordrecht: Reidel), p 27.
10) Sellwood, J.A., Sanders, R.H. 1988. Mon.Not.R.Astron.Soc., 233, 611.
11) Kuijken, K., Gilmore, G. 1989. Mon.Not.R.Astron.Soc., 239, 605.
12) Bahcall, J.N., Flynn, C., Gould, A. 1992. Astrophys.J., 389, 234.
13) Athanassoula, E., Bosma, A., Papaioannou, S. 1987. Astron.Astrophys., 179, 23.
14) Kalnajs, A. 1983. in Internal Kinematics and Dynamics of Galaxies, ed E. Athanassoula (Dordrecht: Reidel), p 87.
15) Buchhorn, M., Mathewson, D.S. 1992. In preparation.
16) Fich, M., Blitz, L., Stark, A. 1989. Astrophys.J., 342, 272.
17) Little, B., Tremaine, S. 1987. Astrophys.J., 320, 493.
18) Norris, J.E., Hawkins, M. 1991. Astrophys.J., 380, 104.
19) Zaritsky, D., Olszewski, E., Schommer, R., Peterson, R., Aaronson, M. 1989. Astrophys.J., 345, 759.
20) Kahn, F., Woltjer, L. 1959. Astrophys.J., 130, 105.
21) Casertano, S., van Gorkom, J. 1991. Astron.J., 101, 1231.
22) Carignan, C., Puche, D. 1990. Astron.J., 100, 394.

23) Carignan, C. 1991. Contribution to Space Telescope Workshop on Dark Matter.

24) Freeman, K.C. 1986. in Nearly Normal Galaxies, ed S. Faber (New York: Springer), p 317.

25) Carignan, C., Freeman, K.C. 1988. Astrophys.J., 332, L33.

26) Carignan, C., Beaulieu, S., Freeman, K.C. 1990. Astron.J., 99, 178.

27) Mateo, M., Olszewski, E., Welch, D., Fischer, P., Kunkel, W. 1991. Astron.J., 102, 914.

28) Pryor, C., Kormendy, J. 1990. Astron.J., 100, 127.

29) Winsall, M.L., Freeman, K.C. 1992. Astron.Astrophys., in press.

30) Fabian, A.C., Thomas, P.A., Fall, S.M., White, R.E. 1986. Mon.Not.R.Astron.Soc., 221, 1049.

31) Hui, X. *et al.* 1992. In preparation.

32) Harris, H.C., Harris, G.L., Hesser, J.E. 1988. in Globular Cluster Systems in Galaxies, ed J.E. Grindlay and A.G.D. Philip (Dordrecht: Kluwer), p 205.

33) Mould, J.R., Oke, J.B., de Zeeuw, P.T., Nemec, J.M. 1990. Astron.J., 99, 1823.

34) Grillmair, C. *et al.* 1992. In preparation.

35) Schweizer, F., van Gorkom, J., Seitzer, P. 1989. Astrophys.J., 338, 770.